Journal of Global Environment Engineering, Vol. 11, pp. 29-44, 2006

WAVE ATTENUATION AND SEDIMENT DEPOSITION DUE TO COASTAL VEGETATION

Toshiyuki ASANO[1]

Abstract

In recent years, it is widely recognized that coastal vegetation may have great value in supporting fisheries, protecting hinterland from wave attack, stabilizing the sea bed and providing good scenery. Hydrodynamic factors play a major role in the functions of water quality, biochemical processes and ecosystems. However, the studies on the hydrodynamics of coastal vegetation, such as wave deformation, sediment movement and bathymetric development, are few and far behind those on the hydrodynamics of riverine vegetation. This paper discusses the recent developments of hydrodynamic models of coastal vegetation focusing on their functions of wave attenuation and sea-bed stabilization.
KEYWORDS: *Coastal vegetation, wave damping, sediment deposition, hydraulic modeling*

1. Introduction

Modern society is becoming increasingly aware of the importance of the environmental preservation of our coastal areas. The environmental value of coastal vegetation is being widely recognized. Coastal vegetation, such as reed forests, algae forests and mangroves, is regarded to perform various useful functions, for example, habitat and feeding ground for fish and marine organisms, maintaining water quality, providing scenic value, etc. Especially, reed wetlands provide attractive scenery often referred to in Japanese poetry and literature and have a valuable role in water purification. In Japan, 1,820 km^2 of algae forests are found, and 600,000 tons of wet weight seaweed is harvested annually. Cultured seaweed in Japan provides 40% of the global production (Nakatani, 1986), which implies that significant portions of our food and nutrition rely on seaweed. Mangrove forests are distributed over 20,000 km^2 in the world. The hydrodynamics in the intricately branched tidal creeks and heavily vegetated flood plains are very unique. The understanding of mangrove creek-swamp systems is important for developing coastal engineering for sub-tropical and tropical regions.

Studies on coastal vegetation have been conducted from wide-ranged aspects such as biological, biochemical, ecological, water quality/sanitary systems. Brix(1994) has summarized various useful functions of wetlands vegetation in relation to the wastewater treatment in constructed wetlands.

For the above-mentioned systems, hydrodynamics play a fundamental role, because the intensity

[1] Dr. Engrg., Professor, Dept. of Ocean Civil Engineering, Kagoshima Univ.,
1-21-40, Korimoto, Kagoshima, 890-0065, JAPAN, Tel. & Fax :+81-99-285-8482
e-mail: asano@oce.kagoshima-u.ac.jp

of the fluid motion and water-exchange rate governs the whole process. As far as the hydrodynamic aspect is concerned, coastal vegetation has the following functions; wave attenuation, protection of the hinterland from wave attack, stabilizing the seabed. In addition, the coastal vegetation is basically flexible, so it does not invite undesirable side effects such as erosions or scouring in the surrounding areas.

To utilize these functions, coastal vegetation is sometimes restored and planted. Restoration projects of native lakeshore environments have been conducted by planting potted young reed plants, for example, in Lake Shinji (Imaoka, 2004), and in Lake Suwa (Hayashi et al., 1999). Broome et al.(1992) transplanted natural cordgrasses for protecting bank erosions in an estuary, and confirmed the performance by conducting a field test. Utilization of coastal vegetation does not always use natural vegetation. For example, artificial seaweed made of polypropylene is manufactured for the purpose of attenuating incoming waves and protecting hinterland. The wave-tank tests and field applications have been reported (Rogers; 1986). The artificial seaweed is also used as a protection facility for local scouring by placing in front of sea-bed structures (Sugahara-Irie, 1990, Sugahara-Nagai, 1994), as a facility for sand depositions and sea-bed stabilizations (Price et al., 1968). Abe et al.(2004) aimed to utilize artificial seaweed as a fish gathering facility focusing on a function of sea-weed beds to generate a sluggish flow zone. They reported that natural algae successfully grew on the eelgrass-shaped substrates, and marine life such as fish and squid are found to be attracted to the substrates.

The success of restoring project of coastal vegetation depends on our understanding on the hydrodynamics of the site, because coastal vegetation is not able to sustain strong wave motions and currents, and also intense sediment movements. For attempts to protect hinterland and stabilize seabed, the understanding of wave attenuation by vegetation is essential. By comparison with the large number of studies in river engineering (Dept. River Engrg. of Ministry of Construction, 1994), where evaluating the roughness effect of vegetation is indispensable to assess the conveyance of the channel, corresponding studies in coastal engineering are scarce.

This study, therefore, intends to summarize the recent studies on the wave attenuation and sediment deposition by the presence of coastal vegetation by referring to the author's studies. The wave hydrodynamics presented here will be fundamental for considering their various environmental functions and for assessing the sustainability of coastal vegetation.

2. A basic theory on wave dumping due to the presence of coastal vegetation

The simplest wave-dumping model is that linear long waves incident to an infinitesimal vegetated area with uniform depth (Figure 1). The x-axis is taken horizontally in the wave propagating direction, and the z-axis is taken vertically to be positively upward from the still water level. The fluid motion receives an additional stress F from the vegetation colony as a reaction of fluid drag force acting on the vegetation. The horizontal momentum equation and the additional stress F are given by,

$$\frac{\partial u}{\partial t} = -g\frac{\partial \eta}{\partial x} - \frac{F}{\rho}, \qquad F = \rho\frac{C_D}{2}N_v d_0 u|u| \tag{1}$$

in which, η is the water surface fluctuation, ρ is the water density, C_D and d_0 is the drag coefficient and diameter of a vegetation stand, respectively, N_v is the number of vegetation per unit area (vegetated density).

To obtain a linear solution, the drag resistance term is quasi-linearized by replacing the first term of the Fourier series, as,

$$\frac{F}{\rho} = \frac{1}{2} C_D d_0 N_v u|u| = \frac{4}{3\pi} C_D d_0 N_v \hat{u} u = Du \tag{2}$$

Combining the following continuity equation with Eq.(1),

$$\frac{\partial \eta}{\partial t} = -h \frac{\partial u}{\partial x} \tag{3}$$

the equation finally becomes as,

$$\frac{\partial^2 \eta}{\partial t^2} + D \frac{\partial \eta}{\partial t} = gh \frac{\partial^2 \eta}{\partial x^2} \tag{4}$$

Assuming the water surface fluctuation η to be sinusoidal,

$$\eta = A_0 \exp(-k_i x) \cos(k_r x - \sigma t) \tag{5}$$

in which, A_0 is the initial wave amplitude, σ is the angular frequency of the wave, k_r, k_i is the real and imaginary part of wave number, respectively. Substituting Eq.(5) into Eq.(4), we have the analytical description for the wave damping coefficient from the imaginary wave number k_i as follows.

$$k_i = \frac{\sigma}{\sqrt{2gh}} \left[\sqrt{1 + (\frac{D}{\sigma})^2} - 1 \right]^{1/2} \approx \frac{\sigma}{2\sqrt{gh}} \left(\frac{D}{\sigma} \right) \tag{6}$$

The approximation yielding the final term is only valid when D/σ is small.

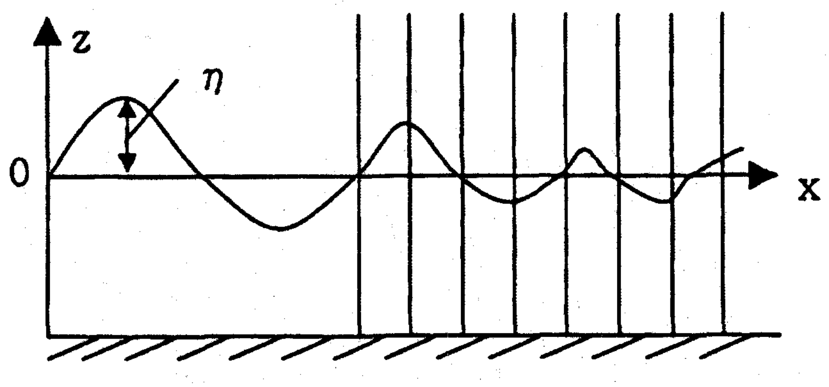

Figure 1 One-dimensional wave propagation model

3. Extension of the theory to realistic situations

For extending the above long wave theory to the shallow water waves, the determination of the quasi-linearized drag coefficient D in Eq. (2) should be modified by considering the vertical velocity distribution as follows;

$$D=\frac{1}{2}C_D d_0 N_v \frac{\overline{\int_{-h}^{0} u^2|u|dz}}{\int_{-h}^{0} u^2 dz} \tag{7}$$

in which, the overbar indicates time averaging over a wave period.

For flexible vegetation like seaweed or reed forests, the drag force may be reduced by swaying response of vegetation stands due to wave actions(Figure 2). In this case, the drag resistance term F should be amended by using the relative velocity u_r between the horizontal fluid velocity u and the swaying velocity of the vegetation stand u_v, $u_r=u-u_v$, as,

$$\frac{F}{\rho}=\frac{1}{2}C_D d_0 N_v u_r|u_r| \tag{8}$$

Asano et al.(1993) modeled the vegetation motion as a forced vibration with one degree of freedom. The motion of a vegetation stand was expressed there as a motion of a cantilever plate possessing a bending stiffness under actions of horizontal fluid forces and buoyancy of the vegetation material. The calculation should start by assuming no vegetation motion $u_v=0$, and then obtain the first step solution for the fluid velocity u. Under the fluid motion, the swaying velocities of the vegetation at any vertical positions u_v are determined. Using the relative velocity $u_r=u-u_v$, the drag resistance term is re-calculated. The computations are repeated until the solution converges.

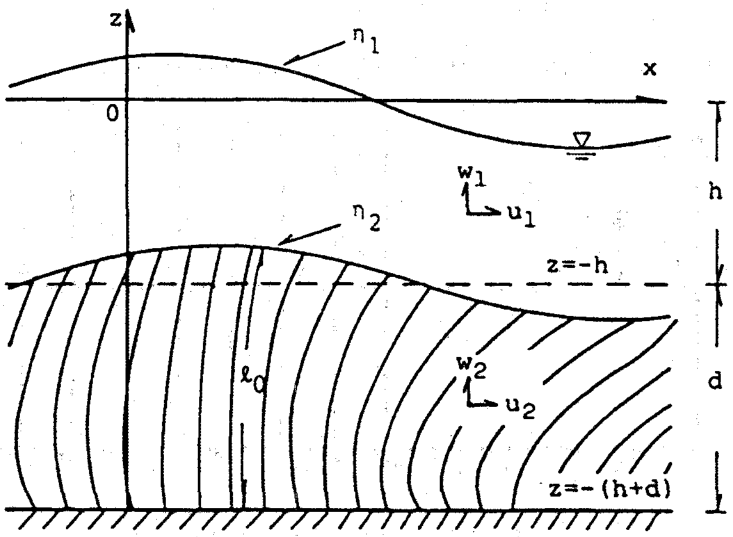

Figure 2 Wave model propagating over flexible vegetation

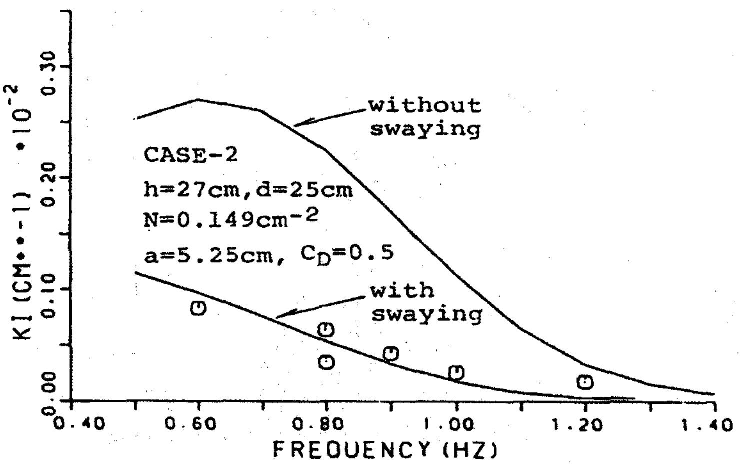

Figure 3 Comparison between measured and calculated wave damping coefficients

For sub-aquatic vegetation, a theoretical model to describe the wave damping including the swaying effects was developed. The validity of the model was confirmed by comparisons with experimental results on wave damping conducted in a 27m long wave tank placing artificial seaweed on the bottom(Asano et al., 1988). Figure 3 illustrates the comparisons between measured and calculated wave damping coefficients plotted against the wave frequencies. The model without considering swaying motion of the vegetation reproduces the measured wave damping only when the drag coefficient C_D of the order 0.1 was used. If the value of C_D=0.5 is given, the model without swaying motion overestimates the wave damping. Whereas, by considering the swaying motion of the vegetation, the improved model is found to provide much better agreement with the same data set, using a more realistic value of the drag coefficient of C_D=0.5.

For mangroves, the roots system has a peculiar configuration (Figure 4). In this case, the drag resistance term should be considered as a function of the vertical coordinate z, because the number of the prop roots per unit area N_v and the diameter d_0 vary with the elevation from the bottom. Several field studies on the mangrove-roots configuration from the aspect of drag resistance are reported (Furukawa-Wolanski, 1996, Mazda et al., 1997, Saad et al., 2001). Mazda et al.(1997) measured the total projected area and volume of mangrove roots system in a control volume, and integrated them to one parameter as an effective tree-trunk spacing L_E. They found that the drag coefficient C_D is well arranged by a Reynolds number using L_E and the value converges towards 0.4 for high Reynolds number.

4. Wave damping propagating into a vegetation fringed channel

(1) Model description

Most existing studies only consider one-dimensional wave problems where the waves propagate into vegetated area with a normal angle. In this section, a quasi- two-dimensional problem is described by introducing our recent model on wave propagations into a vegetation fringed channel(Asano et al., 2005).

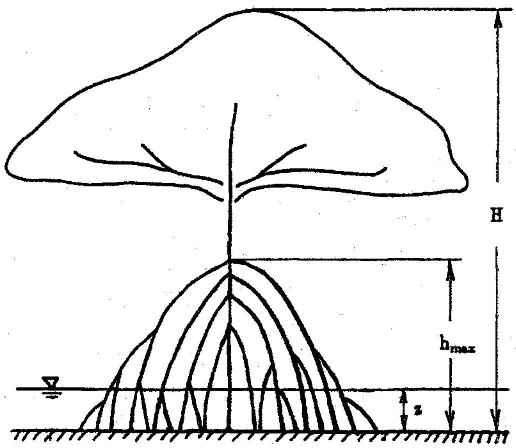

Figure 4 Mangrove roots system

It is observed that waves are attenuated by vegetation flourishing along the banks because momentum exchanges occur between stagnated water mass in the vegetated area and rapidly flowing water mass in the central area. In order to develop an analytical model on the wave attenuation in a vegetation fringed channels, a simple straight channel with uniform depth is assumed (Figure 5). A sinusoidal wave train is normally incident in a straight infinite channel, where vegetation grows over the width B_v along both sides. The horizontal x-axis is taken in the wave propagating direction, and the *y*-axis is taken as the transverse direction and the z-axis is vertical to be positively upward from the still water depth. The water depth h of the channel is assumed to be uniform.

For the numerical model, the following shallow water equations were used to describe the above two-dimensional problem. Numerical models are generally capable of providing the solutions for any complex conditions on vegetation and geometric properties.

$$\frac{\partial \eta}{\partial t}+\frac{1}{n}\frac{\partial}{\partial x}(nM)+\frac{1}{n}\frac{\partial}{\partial y}(nN)=0 \tag{9}$$

$$\frac{\partial M}{\partial t}+c^2\frac{\partial \eta}{\partial x}=-\frac{1}{2}(f_b+f_v)|Q|M/h^2+A_h(\frac{\partial^2 M}{\partial x^2}+\frac{\partial^2 M}{\partial y^2}) \tag{10}$$

$$\frac{\partial N}{\partial t}+c^2\frac{\partial \eta}{\partial y}=-\frac{1}{2}(f_b+f_v)|Q|N/h^2+A_h(\frac{\partial^2 N}{\partial x^2}+\frac{\partial^2 N}{\partial y^2}) \tag{11}$$

in which, c is the wave celerity, n is the group velocity coefficient, M, N is the volume flux for *x*- and *y*- direction, respectively, Q is the composite volume flux given by $Q=\sqrt{M^2+N^2}$. The momentum exchange is herein represented by diffusion terms proportional to the velocity gradient.

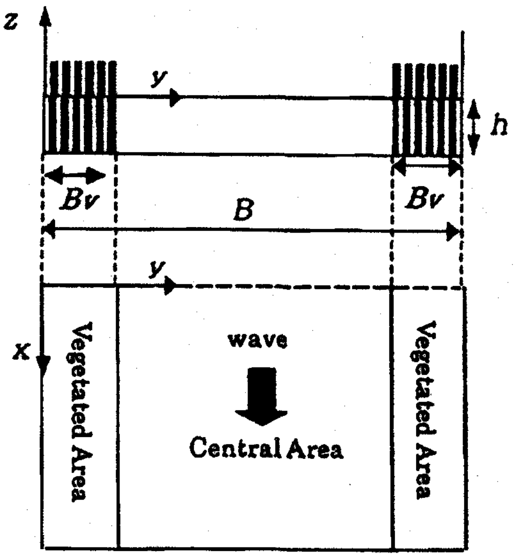

Figure 5 Model of vegetation fringed channel

The horizontal mixing coefficient is defined as A_h, which is herein given by $A_h = 0.05(\Delta x)^{4/3}$ (Δx is the size of the calculation grid). For the bottom friction factor, the symbol f_b is used. The drag coefficient by the vegetation f_v, is presented in terms of the vegetated density N_v, the diameter of a single stand of vegetation d_0, and the drag coefficient C_D, as follows.

$$f_v = C_D \int_{-h}^{0} N_v d_0 \, dz \tag{12}$$

The variables of *M, N* and η are assigned at the staggered grid points and the leap-frog scheme is used in the time direction. A non-reflective boundary scheme proposed by Hino and Nakaza (1988) was adopted at the up-stream boundary to make the computational domain virtually infinite. Figure 6 illustrates a snap shot of wave propagation into the channel. The figure shows that the non-reflective boundary scheme works successfully. The reflection coefficient at the up-stream boundary was found to be less than 10 percent.

Numerical models may be useful because they provide wave solutions for any complex conditions. However, analytical models excel at directly indicating general properties on the wave attenuation. An analytical model on wave attenuation for the channel shown in Fig.-5 is developed. The following momentum equations are proposed; one for the central area (subscript-1) and the other for the vegetated area (subscript-2). At the boundaries of the two areas $y = B_V$, the shear stresses caused by momentum exchanges are considered in terms of a momentum exchange coefficient f_m;

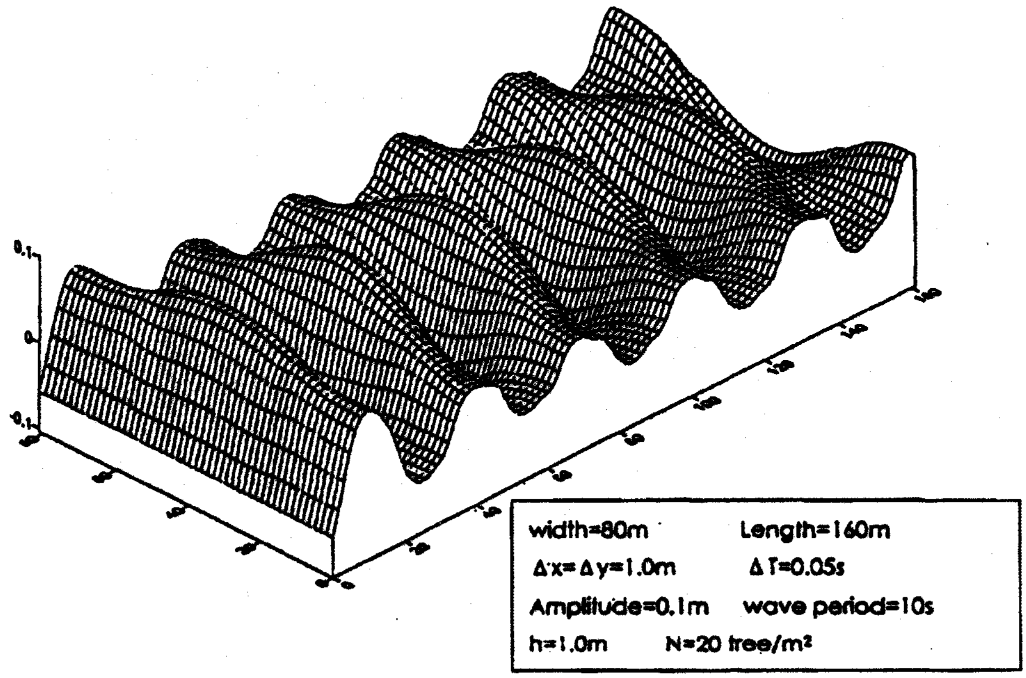

Figure 6 Snap-shot of wave propagation

$$\frac{\partial u_1}{\partial t} = -g\frac{\partial \eta_1}{\partial x} - \frac{f_{b.1}}{2h}u_1|u_1| - \frac{f_m}{h}(u_1-u_2)|u_1-u_2| \tag{13}$$

$$\frac{\partial u_2}{\partial t} = -g\frac{\partial \eta_2}{\partial x} - \frac{f_{b,2}}{2h}u_2|u_2| + \frac{f_m}{h}(u_1-u_2)|u_1-u_2| - \frac{C_D}{2}Nd_0u_2|u_2| \tag{14}$$

The momentum exchange coefficient f_m is also known as the boundary mixing coefficient in river engineering. The suitable values on f_m are proposed for various types of compound channels with vegetated flood planes (Fukuoka-Fujita: 1989).

In order to obtain the linear solution of Eqs. (13) and (14), the quadratic drag resistance terms are linearized likewise Eq. (2); that is, the bottom friction term (the second term in R.H.S. of Eqs.(13),(14)) is presented by $B_i u_i, (i=1,2)$, the drag force term due to vegetation (the last term of Eq. (14)) is Du_i, and the shear stress term generated by the momentum exchanges at the boundary at $y = B_v$ (the third term of R.H.S. of Eqs.(13), (14)) is given by,

$$\frac{f_m}{h}u_r|u_r| = M_i u_i \qquad (i = 1,2) \tag{15}$$

in which, u_r is the relative velocity given by $u_r = u_1 - u_2$. The unknown coefficient M_i can be determined by the condition to minimize the square error $\overline{E^2}_r$ between both sides as

$\partial \overline{E_r^2} / \partial M_i = 0$. Thus, M_i can be evaluated by the following equation,

$$M_i = \frac{f_m}{h} \frac{\overline{u_r |u_r| u_i}}{\overline{u^2_i}} \tag{16}$$

If a sinusoidal variation is assumed for the wave induced velocity, the above equation becomes

$$M_i = \frac{8}{3\pi} \frac{f_m}{h} \frac{\hat{u}_r^2}{\hat{u}_i} \quad (i = 1, 2) \tag{17}$$

Finally, the basic equations are simplified into the following dual one-dimensional linear equations including the interaction effects between the central and vegetated areas by the momentum exchange.

$$\frac{\partial u_1}{\partial t} = -g \frac{\partial \eta_1}{\partial x} - E_1 u_1, \quad (E_1 = B_1 + M_1) \tag{18}$$

$$\frac{\partial u_2}{\partial t} = -g \frac{\partial \eta_2}{\partial x} - E_2 u_2, \quad (E_2 = B_2 - M_2 + D) \tag{19}$$

By coupling with the continuity equation Eq.(3), the analytical expression on the wave damping coefficients $k_{i,i}$ can be obtained by replacing D in Eq.(6) by E_i. By referring the replaced equation, we have found that the bottom friction factor f_b, the drag coefficient C_D, the diameter of a vegetation stand d_0 and the vegetated density N_v increase the wave attenuation rate in roughly proportional way through the term of D; a part of E_2. The angular frequency of the waves σ is found to be cancelled in the final expression, thus the wave period does not affect the attenuation rate as long as the long wave theory is applicable. The attenuation rate varies with the water depth h in inverse proportion to the square root.

(2) Comparisons between analytical and numerical model

Figure 7 depicts the longitudinal variations of wave heights where the initial wave height H_0 is taken as the parameter. The solid curves indicate the numerical results, whereas the dotted curves show the analytical results. Both results show that the wave attenuation rate increases with the initial wave height. This is because the drag resistance term is given to be proportional to the square of the water particle velocity. Wave attenuation is also found in the central area due to the momentum exchange with the vegetated area. These are the common properties found in the numerical and analytical results. However, the decaying figures are different; the exponential decays are found in the analytical results, but not in the numerical results.

Figure 8 shows the effect of the vegetation density N_v. It is commonly observed in both numerical and analytical results that the wave attenuation increases with the vegetation density. In the central area, however, the analytical results are almost independent of N_v, whereas, the numerical results are affected by the change of N_v.

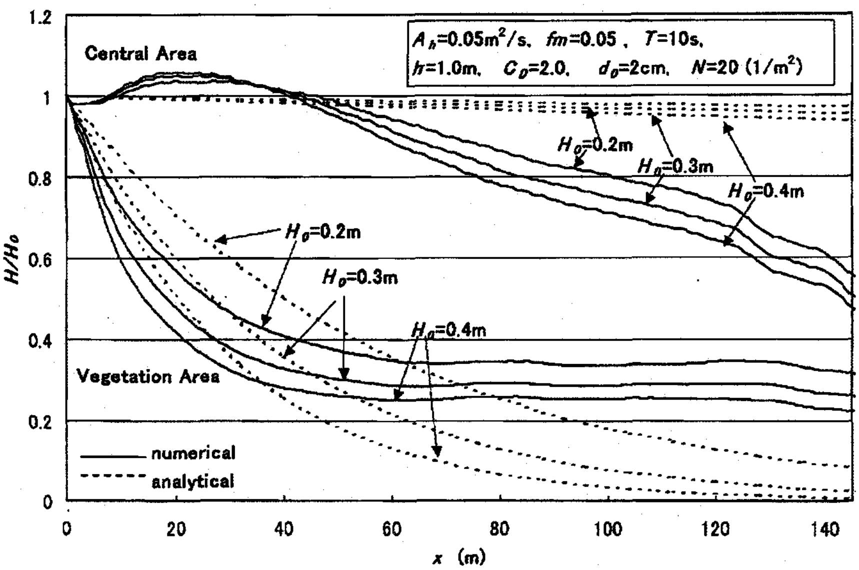

Figure 7 Effects of initial wave height H_0 on wave attenuation

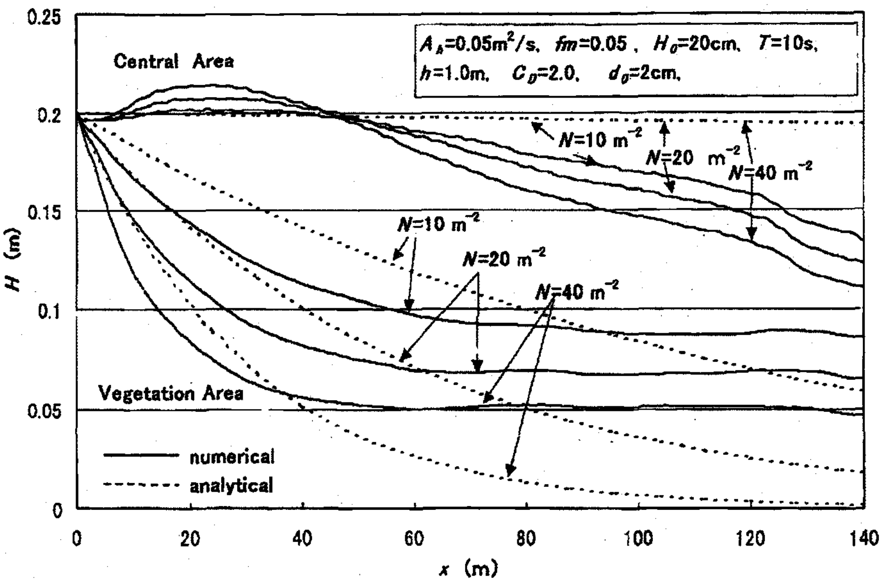

Figure 8 Effects of vegetation density N_v on wave attenuation

Figure 9 illustrates the effects of the horizontal diffusion coefficient A_h for the numerical model, and the momentum exchange coefficient f_m for the analytical model. Both quantities are expressed in different ways, but have the same physical properties. With increase of the horizontal diffusion coefficient, the attenuation obviously increases in the numerical results. Whereas, very little difference is found in the analytical results when the momentum exchange coefficient f_m is varied within the range 0.00～0.15. The effect of f_m only appears for cases waves propagate over a long distance.

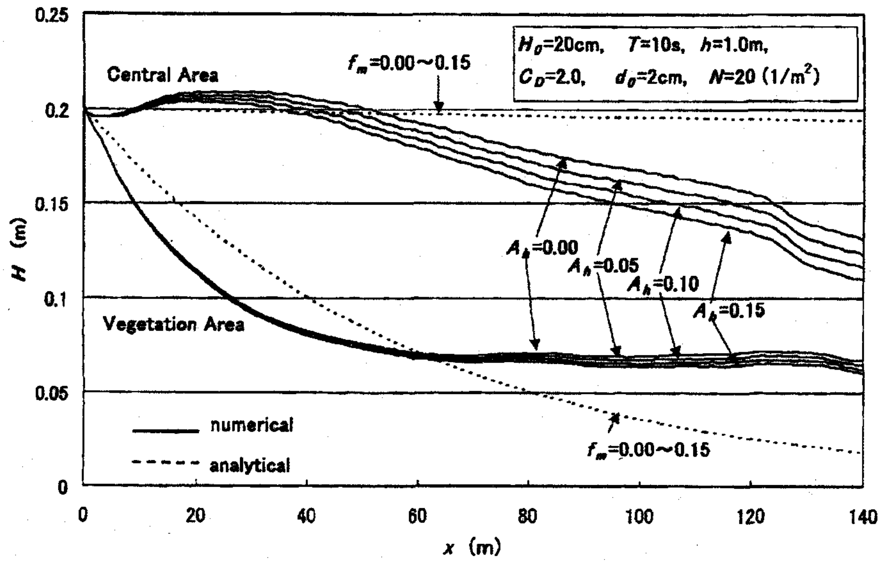

Figure 9 Effects of horizontal diffusion coefficient A_h and momentum exchange coefficient f_m on wave attenuation

Figure 10 shows the effects of the ratio of vegetated area width B_v to the total channel width B. The present analytical model is not able to consider the effect of B_v/B because it is basically a one-dimensional model. Thus, only the numerical results are herein shown. The wave attenuation curves at y=40m are drawn as the representative curves for the central area (note that the total channel width B=80m). Meanwhile, for the vegetated area, those at $y=B_v/2$ are drawn as the representative curves. The wave attenuations are found to increase with the ratio B_v/B not only in the vegetated area but also in the central area.

5. Sediment deposition and self-land creation in coastal wetlands

In tidal inlets and fluvial plains, turbulent water enters into vegetated areas at flood tide. High turbulence will be generated by vegetation stems/roots system, keeping the fine sediment in suspension. Sedimentation occurs during the period of the slack tide, when the turbulence vanishes and sediment will deposit on the bottom. Furukawa and Wolanski (1996) pointed out that mangrove forests have such "pump-up" function of fine sediment from coastal water to the mangrove area. For river channels, Fujita et al.(1996) investigated the wash load deposition and resultant channel narrowing due to vegetation growing in the flood-plain. These studies show that vegetation community has a geomorphic role through sediment trapping. In other words, for designing an equilibrium cross section of a channel or for proper planning on vegetated wetland construction, the understanding on the sediment trapping ability of the vegetation is vitally important.

Located in the inter-tidal area, vegetation community is potentially not very stable and may be altered by the future sea level rise. Several studies show that the rise of sea level will affect estuary and inter-tidal systems (Ellison-Stoddart ; 1992). However, the vegetation community may have an ability to counteract the impact of sea level rise through their lateral and vertical growth via sediment accretion.

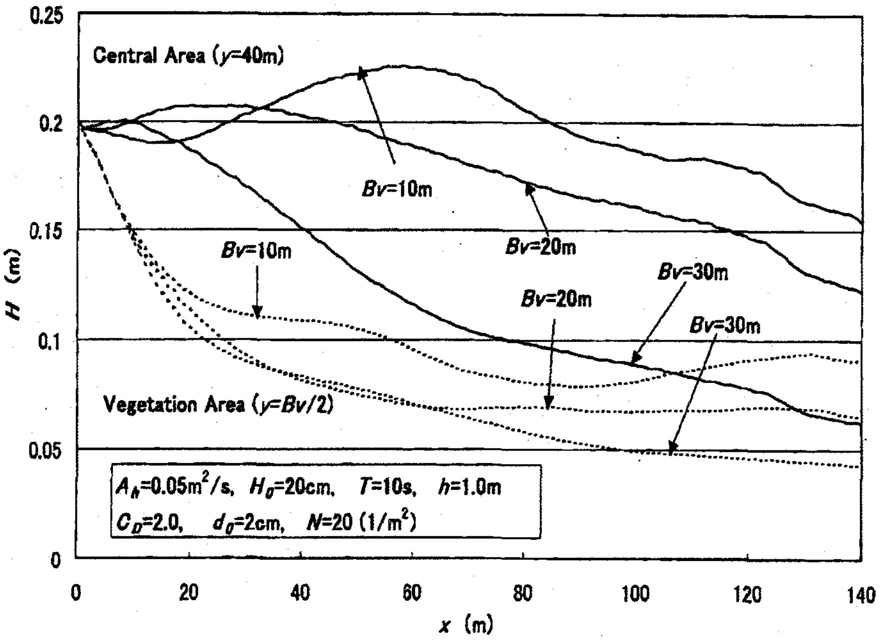

Figure 10 Effects of relative width of vegetation area B_V/B on wave attanuation

Saad et al.(1999) investigated the sediment pump-up mechanism and evaluated the yearly rise of the mud-bed substrate in a mangrove estuary in Malaysia. They measured the accretion rates and sediment characteristics monthly over two years. The accretion rates were evaluated from the temporal variations of ground levels, which were monitored in total 116 stations locating along 7 transects in the flood-plane perpendicular to the estuaries. The observed accretion rates, although much scattered, show a common tendency for all the measuring transects as that the rates become the highest at the edge of mangrove area facing the channel, then decrease towards the back mangrove area (Figure 11). The higher accretion rates near the mangrove edge may result from longer exposed time of tidal inundation. The monthly accretion rates are found to be predominant in monsoon season, because large rainfalls and flooding from the upstream of the estuary convey a great amount of sediment. After all, the over-all average accretion rate was found to be 1.06cm/year in the site, which were comparable to the existing accretion rates surveyed in mangrove forests and salt marsh wetlands (Table-1). The accretion rate is about double of the predicted future sea level rise of 0.5cm/year, which suggests that the mangrove forest systems may mitigate the impact of sea level rise.

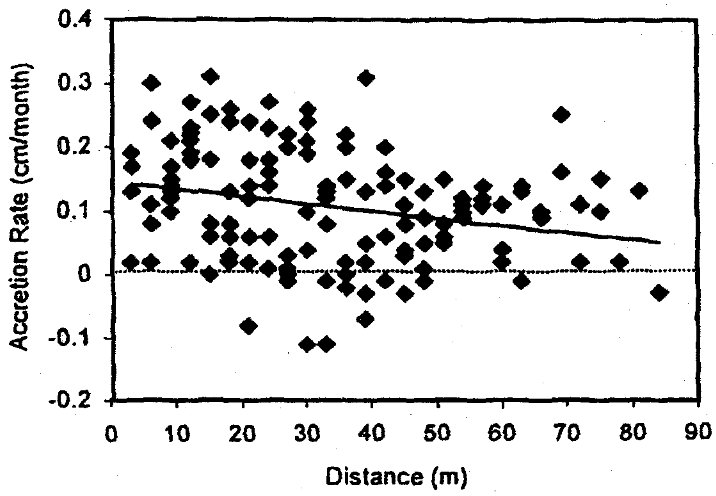

Figure 11 Relationship between sediment accretion rates and distance from mangrove edge

Table 1 Existing measurements on sediment accretion rates in mangrove forests and salt marsh wetlands

Study	Method	Accrealion Rat (cm/yr)	Location
Chapman & Ronaldson (1958)	Brick-dust marker	0.1	New Zealand Salt Marsh
Bird (1971)	Stake	0.8	*Avicennia* forest Southern Australia
Harrison & Bloom (1977)	Artificial marker Horizon	0.2 - 0.5	Connecticut *S. patens* marsh
Armentano & Woodwell (1975)	^{210}Pb	0.47 - 0.63	Long Island, NY Flax pond, *S. alterniflora*
Spenceley (1977, 1982)	Grids of Stakes	0 46	*Avicennia* North Earth Australia
DeLaune *et al.* (1978)	^{137}Cs	1.35 0 75	Barataria Basin LA
Stevenson *et al.* (1985)	^{210}Pb	0 17 - 0.36	Chesapeake Bay
Onema & DeLaune (1988)	^{137}Cs	1.0 1.5	Rattekaai, salt marsh St. Annaland, salt marsh
Lynch *et al* (1989)	^{210}Pb and ^{137}Cs isotopes	0.3	Mexico, mangrove
Woodroffe (1990)	Radiocarbon	0.6	Northern Australia mangrove
French & Spencer (1993)	Artificial marker Honzon	0.56	Norfolk, U.K
Leonard *et al.* (1995)	Sediment traps	0.12 - 0.76	West-central FL *J. roemrianus* (Cedar Creek)
Saad et al. (1999)	Artificial marker horizon	0.64 -1.46	East coast of Peninsular Malaysia, mangrove

6. Conclusions

The purpose of this paper is to present a review of the hydrodynamics of coastal vegetation focusing on its functions of wave attenuation and sediment deposition.

The first section introduced the various environmental values of coastal vegetation, and stressed the importance of preservation. Next, as a basis of hydrodynamics, the simplest wave-damping model was presented. The third section was devoted to describing the extension of the mathematical models which can be used in more realistic situations.

The wave-damping model propagating into a vegetation fringed channel was shown in the next section. Analytical and numerical analyses were developed and the effects of the wave and vegetation properties on the wave attenuation were investigated. Both analytical and numerical results revealed that the wave attenuation rate is dependent on the initial wave height because the drag resistance by the vegetation is quadratic to the wave particle velocity. The analytical model has the merit of showing that the wave attenuation characteristics are clearly indicated in the solution. However, the analytical model is a one-dimensional model, even though the momentum exchanges between the central and vegetated area are considered. The model has a certain limit for describing two dimensional effects such as the effect of the relative width of the vegetated area.

Attenuation of waves and currents due to the vegetation will generate slack flow areas and result in sediment deposition in the vegetated areas. In the final section, sediment accretion rates in coastal wetlands were investigated by referring to existing field observations including the authors' field survey. The accretion rates are generally greater than the rate of the predicted sea level rise, which suggests mangrove and salt marsh systems may mitigate the impact of the sea level rise.

In conclusion, as far as the hydrodynamic aspects are concerned, it is basically possible to solve any expected problems by using mathematical and numerical models, because highly non-linear wave theories are not necessary to describe the flow fields. However, there still remain several problems such as how to quantify suitable values for the model parameters. Accumulation of reliable field data to verify the mathematical models is required. For the restoration and management of coastal vegetation, it is not sufficient to consider only from the hydrodynamic aspects. Understanding of the bio-chemical and ecological aspects is also essential to sustain the conditions for the vegetation growth.

Acknowledgements

The author would like to express his appreciation to the former Kagoshima Univ. students Dr. Shahbudin Saad, Ms. Ryoko Matsumoto for their cooperation in the field and numerical works. He also would like to express his thanks to Mr. Seiji Kikuchi, Shinki Corp., for his valuable comments.

References

Abe, F., D. Edagawa, S. Kikuchi, H. Maruta and K. Yamaoka(2004): Eelgrass-shaped substrate for the growth of algae and its ability to attract marine life, Suisanzoshoku, Vol.52, pp.109-120.

Asano, T., S. Tsutsui and T. Sakai (1988): Wave damping characteristics due to seaweed, Proc. 35th Conf. on Coastal Engrg., pp.138-142(in Japanese).

Asano, T. , H. Deguchi and N. Kobayashi (1993): Interaction between water waves and vegetation, Proc. of 23rd Inter. Conf. of Coastal Engrg., ASCE, Vol.3, pp.2710-2723.

Asano, T., R. Matsumoto and S. Kikuchi(2005): Wave deformations in vegetation fringed channels, Proc. 29th Inter. Conf. of Coastal Engrg., ASCE , vol.1, pp.218-229.

Brix, H.(1994):Functions of macrophytes in constructed wetlands, Water Science & Technology, Vol.29, No.4, pp.71-78.

Broome, S., S. M. Rogers and E. D. Seneca (1992): Shoreline erosion control using marsh vegetation and low-cost structures, Sea Grant Pub. of U.S. Environmental Protection Agency and Univ. North Carolina, 20p.

Dean, R. G. and R. A. Dalrymple (1991): Long waves with bottom friction, Water Wave Mechanics for Engineers and Scientists, World Scientific, 353p., pp.146-154.

Dept. River Engrg., Ministry of Construction (1994): Guideline for cut-down and planting trees in river channels, Sankaido Pub. Co., 144p(in Japanese).

Ellison, J.C. and Stoddart, D. R.(1992): Mangorve ecosystem collapses with predicted sea level rise, Holocene analogues and implications, J. Coastal Research, Vol.7, pp.151-165.

Fujita, K., J.A. Moody, T. Uda and M. Fujii(1996): Accretion of flood-plains by wash load deposit and resulting channel narrowing, J. of Hydraulic, Coastal and Environmental Engineering, JSCE, No.551, II-37, pp.47-62.

Fukuoka, S. and K. Fujita (1989): Prediction of flow resistance in compound channels and its application to design of river courses, Journal of Hydraulic, Coastal and Environmental Engineering, JSCE, Vol.411, II-12, pp.63-72(in Japanese).

Furukawa, K. and E. Wolanski (1996): Sedimentation in mangrove forest, Mangrove and Salt Marshes, Vol.1, pp.3-10.

Hayashi, K. Y. Kimura, M. Suzuki, K. Hagiwara and T. Shigemura (1999): Effect of reed hedges on bank protection in lakes, Proc. of Coastal Engineering, JSCE, pp. 1116-1120(in Japanese).

Hayashi,K., Y. Takahashi and T. Shigemura (2002): Wave forces and transmitted waves on plants in lake and coast, Proc. of Coastal Engineering, JSCE, pp.721-725(in Japanese).

Hino, M. and E. Nakaza (1988) : Application of a new non-reflecting boundary scheme for numerical wave analysis to plane two dimensional problems, Proc. of Japanese Conference on Coastal Engineering, Vol. 35, pp.262-266(in Japanese).

Imaoka, T. (2004): A lakeshore restoration project on the western shore of Lake Shinji, Inter. Seminar on Restoration of Damaged Lagoon Environments, Poster Session PA3.

Izumi, N. and S. Ikeda(1989) : Stable channel cross-section of straight gravel rivers with trees on banks, Journal of Hydraulic, Coastal and Environmental Engineering, JSCE, Vol.411, II-12, pp.151-160(in Japanese).

Mazda, Y., et al. (1997): Drag force due to vegetation in mangrove swamps, Mangrove and Salt Marshes, Vol.1, pp.193-199.

Nakatani, S. (1986): Perspectives of creating algal beds in Japan, Bulletin on Coastal Oceanography, Vol.24, No.1, pp.40-52.

Price, W.A., K.W. Tomlinson and J. N. Hunt(1968): The effect of artificial seaweed in promoting the build up of beaches, Proc. 11th Inter. Conf. of Coastal Engrg., pp.570-578.

Rogers, S.(1986): Artificial seaweed for shoreline erosion control, UNC Sea Grant Pub., UNC-SG-WP-8-6-4, Univ. of North Carolina, p.15.

Saad, S., M. Lokman Husain, N. A. M. Shazili and T. Asano (1999): Sediment accretion and variability of sedimentological characteristics of a tropical estuarine mangrove: Kemaman, Terengganu, Malaysia, J. of Mangrove and Salt Marshes, Vol. 3, No. 1, pp.51-58.

Saad, S., T. Asano and M. Lokman Husain (2001): Tidal flow simulations in a mangrove estuary comprised of branched creeks and vegetated flood plains, Asian and Pacific Coastal Engineering, pp.956-965.

Sugahara, K. and I. Irie (1990) : Experiments on the effects of artificial seaweed on the sand movement, Tech. Note of the Port and Harbour Research Inst., No.692, pp.1-48.

Sugahara, K. and T. Nagai(1994): Hydraulic model experiment on the artificial seaweed against scouring and beach erosion, Technical Note of the Port and Harbor Research Inst., No.771, pp.1-39.